Interaction between CD9 and PI3K-p85 activates the PI3K/AKT signaling pathway in B-lineage acute lymphoblastic leukemia

YI-FEN SHI[1*], ZI-YANG HUANG[1*], YI-SHA HUANG[1], RU-JIAO DONG[1], CHONG-YUN XING[1], KANG YU[1], KAM TONG LEUNG[2] and JIAN-HUA FENG[1,3]

[1]Department of Hematology, The First Affiliated Hospital of Wenzhou Medical University, Wenzhou, Zhejiang 325000; [2]Department of Paediatrics, The Chinese University of Hong Kong, Shatin, Hong Kong, SAR 999077; [3]Department of Pediatrics, The First Affiliated Hospital of Wenzhou Medical University, Wenzhou, Zhejiang 325000, P.R. China

Received August 7, 2020; Accepted April 21, 2021

DOI: 10.3892/or.2021.8091

Abstract. Our previous study has shown that *CD9* knockdown could suppress cell proliferation, adhesion, migration and invasion, and promote apoptosis and the cytotoxicity of chemotherapeutic drugs in the B-lineage acute lymphoblastic leukemia (B-ALL) cell line SUP-B15. In this study, we further investigated the molecular mechanism underlying the effects of CD9 on leukemic cell progression and the efficacy of chemotherapeutic agents in B-ALL cells. Using the CD9-knockdown SUP-B15 cells, we demonstrated that the silencing of the *CD9* gene significantly reduced the expression of phosphorylated-phosphatidylinositol-3 kinase (p-PI3K), phosphorylated-protein kinase B (p-AKT), P-glycoprotein (P-gp), multidrug resistance-associated protein 1 (MRP1), breast cancer resistance protein (BCRP), matrix metalloproteinase 2 (MMP2) and phosphorylated-focal adhesion kinase (p-FAK). In addition, glutathione S-transferase (GST) pull-down assay showed the binding between CD9 and both PI3K-p85α and PI3K-p85β *in vitro*, while co-immunoprecipitation assay showed the binding between CD9 and both PI3K-p85α and PI3K-p85β *in vivo*. Furthermore, the PI3K/AKT inhibitor LY294002 mirrored the effects of *CD9* knockdown in SUP-B15 cells. Taken together, these findings demonstrated that CD9 activates the PI3K/AKT signaling pathway through direct interaction with PI3K-p85 in B-ALL cells. Our data provide evidence for the inhibition of the PI3K/AKT pathway as a novel therapeutic option in CD9 antigen-positive B-ALL.

Correspondence to: Dr Jian-Hua Feng, Department of Hematology, The First Affiliated Hospital of Wenzhou Medical University, 2 Fuxue Road, Wenzhou, Zhejiang 325000, P.R. China
E-mail: wzfjh@126.com

Dr Kam Tong Leung, Department of Paediatrics, The Chinese University of Hong Kong, Ma Liu Shui, Shatin, Hong Kong, SAR 999077, P.R. China
E-mail: ktleung@cuhk.edu.hk

[*]Contributed equally

Key words: B-lineage acute lymphoblastic leukemia, CD9, PI3K-p85, PI3K/AKT signaling pathway, SUP-B15 cells

Introduction

CD9, a member of the tetraspanin superfamily, is a cell surface glycoprotein with a molecular weight of 24-27 kDa (1). Recent studies have shown that CD9 is expressed in 72% of adult B-lineage acute lymphoblastic leukemia (B-ALL) (2) and 78% of pediatric B-ALL (3) and correlates with leukemia progression and clinical survival. Initially in 2009 and 2011, Nishida *et al* and Yamazaki *et al* reported that the CD9 antigen-positive ($CD9^+$) B-ALL cell population possessed stem cell characteristics within the clone; $CD9^+$ B-ALL cells were relatively more resistant to chemotherapeutic agents than $CD9^-$ cells (4,5). In 2015, Arnaud *et al* identified that CD9 promoted the activation of Ras-related C3 botulinum toxin substrate 1 (RAC1) and enhanced C-X-C motif chemokine receptor 4-mediated migration and engraftment of B-ALL cells to the bone marrow or testis (6). In 2018, Liang *et al* demonstrated that $CD9^+$ acute lymphoblastic leukemia (ALL) patients exhibited a higher positive rate of the *BCR-ABL* fusion gene compared with $CD9^-$ patients, and CD9 expression was related to poor prognosis in ALL patients (2). In 2019, Leung *et al* reported that $CD9^+$ B-ALL children had a significantly lower 5-year relapse-free survival rate than $CD9^-$ patients; the administration of anit-CD9 antibody suppressed leukemia progression in NOD/SCID mice xenografted with $CD9^+$ cell lines and primary B-ALL blasts from high-risk and refractory patients; the blockage of CD9 inhibited B-ALL cell proliferation, induced cell cycle arrest and promoted chemotherapeutic agent-induced apoptosis (3). Furthermore, our recent study demonstrated that the downregulation of CD9 inhibited cell proliferation, adhesion, migration and invasion, while increasing apoptosis and the cytotoxicity of chemotherapeutic agents in B-ALL SUP-B15 cells (7). Therefore, CD9 serves an important role in the disease progression and clinical prognosis in B-ALL. Nevertheless, the corresponding mechanisms remain to be explored.

It is well known that the activation of the phosphatidylinositol 3-kinase (PI3K)/serine/threonine-specific protein kinase (AKT) signaling pathway plays an important role in tumorigenesis and development. The PI3K/AKT signaling pathway has been shown to be involved in a variety of tumor-related biological functions, such as cell survival, apoptosis resistance, drug resistance and metastasis (8). Emerging evidence has also revealed that tetraspanin proteins could regulate the PI3K/AKT signaling pathway. For example, the integrin α3β1-tetraspanin protein complexes have been implicated in actin cytoskeletal reorganization via a PI3K-dependent mechanism (9). In addition, the ectopic expression of the tetraspanin CD151 had a negative regulatory effect on AKT activation (10). Furthermore, it has been reported that interleukin (IL)-16 could activate the PI3K signaling pathway by binding to CD9 in mast cells (11). Considering the above findings, it is hypothesized that CD9 might be involved in the regulation of the biological behavior of B-ALL cells through the PI3K/AKT pathway.

Therefore, the aims of the present study were: i) To investigate the relationship between CD9 and the PI3K/AKT pathway; and ii) to assess the *in vitro* anti-leukemia effects mediated by inhibition of the PI3K/AKT pathway in $CD9^+$ B-ALL cells.

Materials and methods

Cell lines and culture conditions. Cell lines SUP-B15 and 293T were purchased from The American Type Culture Collection (ATCC). The SUP-B15 cell line was authenticated by short tandem repeat DNA profiling analysis at Suzhou Genetic Testing Biotechnology Corporation, China. SUP-B15 cells were cultured in Iscove's modified Dulbecco's medium (IMDM) with 20% fetal bovine serum (FBS), and 293T cells were cultured in Dulbecco's modified Eagle's medium (DMEM) with 10% FBS. All cells were maintained in a humidified incubator at 37˚C in an atmosphere of 5% CO_2.

Short hairpin RNA (shRNA) lentiviral transduction. The transduction protocols were described in our previous paper (7). Briefly, 12 μg PHY-310 lentiviral vector (hU6-MCS-CMV-ZsGreen1-PGK-Puro; Shanghai Hanyin Biotechnology Co., Ltd.) containing an shRNA targeting *CD9* [the target sequence for *CD9* shRNA: 5'-AGGAAGTCCAGGAGTTTTA-3' (synthesized by Shanghai Hanyin Biotechnology Co., Ltd.); primers used for targeting the interference sequence of the *CD9* gene: F: GATCCAGGAAGTCCAGGAGTTTTATTCAAGAGATAAAACTCCTGGACTTCCTTTTTTTG and R: AATTCAAAAAAAGGAAGTCCAGGAGTTTTATCTCTTGAATAAAACTCCTGGACTTCCTG) and 9 μg lentiviral packaging vector LV-PV001 [a second-generation packaging vector; Han Yin Biotechnology (Shanghai) Co., Ltd.] were mixed with polyethylenimine (Sigma-Aldrich; Merck KGaA) and incubated for 20 min at 37˚C. Then, the subconfluent 293T cells ($1.5x10^8$/dish) in a 10-cm culture dish were transfected with the transfection mixture. The blank PHY-310 vector (in order to exclude the effect of the lentiviral vector on the experimental results) was used as a negative control. At 48 h after transfection, lentiviral particles produced from the transfected 293T cells were harvested and purified by ultra-centrifugation at 3,000 x g for 2.5 h at 4˚C. SUP-B15 cells were transduced with the lentiviral particles [multiplicity of infection (MOI)=100)] by centrifugation in the presence of 8 μg/ml polybrene (Sigma-Aldrich; Merck KGaA) at 37˚C for 4 h, and then stable cell lines were generated by selection with puromycin (1 μg/ml) for 48 h. The efficiency of *CD9* knockdown was evaluated by reverse transcription-quantitative PCR (RT-qPCR). The method of RT-qPCR was carried out according to a previous study (7).

Enzyme linked immunosorbent assay (ELISA). The levels of phosphorylated-PI3K (p-PI3K) in SUP-B15 cells were measured using the Human p-PI3K ELISA kit (cat. no. M1060625; Shanghai Enzyme-linked Biotechnology Co., Ltd.) according to the manufacturer's protocol. Briefly, cells were lysed by three consecutive freeze-thawing cycles (10 min each), and then centrifuged at 860 x g for 10 min at 4˚C. The total protein concentration in the supernatant was determined using a BCA protein assay kit (Beyotime Institute of Biotechnology). Subsequently, 50 μl of total protein extraction (1:5 dilution with PBS) or standards along with 50 μl of biotin-labeled anti-p-PI3K antibody were incubated on an antibody-coated plate for 1 h at 37˚C. Wells were then washed three times. The next step involved adding 80 μl of streptavidin-labeled horseradish peroxidase (HRP) to each well, followed by incubation at 37˚C for 30 min. After washing for three times, 50 μl of substrate solution A along with 50 μl of substrate solution B was added to each well and the plate was incubated at 37˚C for 10 min. The reaction was quenched by the addition of 50 μl of stop solution. The plate was analyzed by evaluating the absorbance at 450 nm using a Spectra MAX M5 microplate reader (Molecular Devices).

Western blot analysis. The methods of protein extraction and western blotting were carried out as previously described (7). Briefly, cells were lysed using RIPA lysis buffer (Beyotime Institute of Biotechnology) and the total protein concentration was measured by the BCA protein assay kit (Beyotime Institute of Biotechnology). Total protein was then separated by 10% sodium dodecyl sulfate-polyacrylamide gel electrophoresis (SDS-PAGE) and transferred to a PVDF membrane. The membranes were blocked with 5% skim milk for 1 h at room temperature, and sequentially incubated overnight with primary antibodies at 4˚C. The primary antibodies used were anti-phosphorylated-AKT (anti-p-AKT; 1:1,000 dilution, cat. no. 9018; Cell Signaling Technology, Inc.), anti-AKT (1:1,000 dilution, cat. no. 2938; Cell Signaling Technology, Inc.), anti-p53 (1:1,000 dilution, cat. no. CY5131; Abways, Inc.), anti-p21 (1:1,000 dilution, cat. no. CY5088; Abways, Inc.), anti-cleaved caspase 3 (1:1,000 dilution, cat. no. CY5051; Abways, Inc.), anti-P-glycoprotein (anti-P-gp; 1:1,000 dilution, cat. no. 13978; Cell Signaling Technology, Inc.), anti-multidrug-resistance associated protein 1 (anti-MRP1; 1:1,000 dilution, cat. no. CY6878; Abways, Inc.), anti-breast cancer resistance protein (anti-BCRP; 1:1,000 dilution, cat. no. 10051-1-AP, ProteinTech Group, Inc.), anti-matrix metalloproteinase 2 (anti-MMP2; 1:1,000 dilution, cat. no. BS1236; Bioworld Technology, Inc.), anti-phosphorylated-focal adhesion kinase (anti-p-FAK; 1:1,000 dilution, cat. no. CY6207; Abways, Inc.), anti-FAK (1:1,000 dilution, cat. no. CY5464; Abways, Inc.) and

anti-β-actin (1:5,000 dilution, cat. no. ab2001; Abways, Inc.). Following incubation using HRP-conjugated anti-rabbit antibody (1:10,000 dilution, cat. no. 7074P2; Cell Signaling Technology, Inc.) or HRP-conjugated anti-mouse antibody (1:10,000 dilution, cat. no. 7076; Cell Signaling Technology, Inc.) at room temperature for 2 h, the protein bands were analyzed with chemiluminescent solution (ECL Western Blotting Detection Reagents; GE Healthcare Life Sciences). The relative level of protein expression was quantified by ImageJ software (version 1.49p; National Institutes of Health) and standardized to β-actin levels.

Cell proliferation assay. The cell proliferation was determined by use of a Cell Counting Kit-8 (CCK-8; Dojindo Molecular Technologies, Inc.). Cells were cultured in 96-well microplates at a density of $3x10^3$ cells/well. After incubation at 37˚C for 24, 48, 72, 96 and 120 h, 10 μl of CCK-8 solution was added to each well and the cells were incubated at 37˚C for 2 h. The absorbance was measured at 450 nm using a Spectra MAX M5 microplate reader (Molecular Devices).

Drug sensitivity assay. The measurement of *in vitro* drug sensitivity to chemotherapeutic agents were carried out according to our previous study (7). Cells were exposed to various concentrations of chemotherapeutic agents, including vincristine (VCR; Selleck Chemicals), daunorubicin (DNR; MedChemExpress), cyclophosphamide (CPM; MedChemExpress) and dexamethasone (DXM; Selleck Chemicals), at 37˚C for 48 h, and then CCK-8 assay was used to detect the cell viability. The optical density (OD) was measured at 450 nm using a Spectra MAX M5 microplate reader (Molecular Devices). The percentage of cytotoxicity was calculated by the following formula: Cytotoxicity (%)=(1-mean OD of treated/mean OD of control) x100.

Cell adhesion assay. An artificial basement membrane was prepared by adding 0.5 μg Superfibronectin (Sigma-Aldrich; Merck KGaA) into each well of a 96-well plate and incubating at 4˚C overnight. Subsequently, a total of $1x10^5$ cells resuspended in 200 μl IMDM medium was seeded into each well of a 96-well plate and allowed to adhere to the Superfibronectin at 37˚C for 90 min in a humidified 5% CO_2 atmosphere. Non-adherent cells were removed by rinsing with PBS and adherent cells were then quantified by CCK-8 assay.

Cell migration and invasion assays. For the cell migration assay, a total of $1x10^4$ cells in serum-free IMDM medium (100 μl) was placed in the upper chamber of an 8-μm pore size Transwell plate (Corning, Inc.) and 800 μl of IMDM medium containing 10% FBS was added to the lower chamber as a chemoattractant. After incubation for 72 h at 37˚C in a 5% CO_2 atmosphere, cells that migrated to the lower chamber were harvested and stained with 1% crystal violet at room temperature for 30 min after fixation with 4% paraformaldehyde at room temperature for 20 min. Finally, a hemocytometer was used to count the cells under a light microscope (magnification, x100). The invasion assay was performed using the same method as the migration assay, except for the precoating of the upper chamber with 50 μl Matrigel (1 mg/ml; BD Biosciences) at 37˚C for 5 h.

Plasmid construction. The full-length cDNA of *CD9* was cloned into the mammalian expression plasmid pcDNA3.1-Flag-MYC (Gene Universal), forming a MYC tagged CD9 expression vector pcDNA3.1-MYC-CD9, while full-length cDNA of PI3K-p85α or PI3K-p85β was inserted into pcDNA3.1-Flag-HA (Gene Universal), forming a HA tagged PI3K-p85α expression vector pcDNA3.1-HA-p85α or PI3K-p85β expression vector pcDNA3.1-HA-p85β. The empty plasmids, pcDNA3.1-Flag-MYC and pcDNA3.1-Flag-HA, were used as negative control groups. Vector pET28 (Gene Universal) was used to construct vectors expressing glutathione S-transferase (GST)-p85α or GST-p85β fusion proteins.

GST pull-down assay. MYC-CD9 expression vector (2.5 μg) was mixed with Lipofectamine 2000 transfection reagent (Thermo Fisher Scientific, Inc.) and incubated for 20 min at 37˚C. Then, 293T cells in 10-cm dishes were grown to 90% confluence and transfected with the mixture. At 48 h after transfection, the cells were harvested and lysed by RIPA lysis buffer (Beyotime Institute of Biotechnology). After centrifugation at 16,560 x g for 15 min at 4˚C, the supernatants were isolated. On the other hand, BL-21 bacterial cells were transformed with plasmids encoding the GST-tagged proteins and then grown at 37˚C until reaching log phase. GST protein expression was induced by incubation with isopropyl-1-thio-β-galactopyranoside (IPTG; 1 mmol/l) for 6 h. In order to purify the GST fusion proteins, cells were lysed by sonication in lysis buffer [50 mmol/l Tris (pH 7.4), 150 mmol/l NaCl and 1% NP-40], and the resulting lysate was incubated for 1 h at 4˚C with glutathione-agarose beads (cat. no. G4510; Sigma-Aldrich; Merck KGaA). The beads were harvested by centrifugation and washed with lysis buffer.

For CD9 binding, 50 μl of whole cell lysate from transfected 293T cells were incubated for 48 h with the GST-tagged proteins bound to beads. Unbound CD9 protein was removed by three washes with lysis buffer (1 ml each). Bound proteins were eluted by boiling in 1X loading buffer, separated by 10% SDS-PAGE, and examined by immunoblot analysis with anti-MYC antibody (1:1,000 dilution; cat. no. A7470; Sigma-Aldrich; Merck KGaA).

Co-immunoprecipitation assay. MYC-CD9 expression vector (2.5 μg) and either 2.5 μg of HA-PI3K-p85α or HA-PI3K-p85β expression vector were mixed with Lipofectamine 2000 transfection reagent (Thermo Fisher Scientific, Inc.) and incubated for 20 min at 37˚C. Then, 293T cells in 10-cm dishes were grown to 70-90% confluence and transfected with the mixture. At 48 h after transfection, the cells were harvested and lysed by RIPA lysis buffer (Beyotime Institute of Biotechnology). Following the centrifugation using the same method described previously, the supernatants were isolated and immunoprecipitated with 5 μl anti-MYC antibody (cat. no. A7470; Sigma-Aldrich; Merck KGaA). Detection of the co-precipitated HA-PI3K-p85α or HA-PI3K-p85β was performed using western blotting by incubating with an anti-HA antibody (1:1,000 dilution, cat. no. ab49969; Abcam, Inc.). The supernatants described above were also subjected to direct western blot analysis to confirm the expression of MYC-CD9 and either HA-PI3K-p85α or HA-PI3K-p85β.

In vitro anti-leukemia effects of the PI3K/AKT pathway inhibitor in SUP-B15 cells. SUP-B15 cells ($5x10^3$) were treated with the PI3K/AKT pathway inhibitor LY294002 (0.6 μmol/l; cat. no. HY-10108, MedChemExpress) at 37˚C for 24 h, and then subjected to cell proliferation, drug sensitivity, adhesion, migration, invasion, ELISA and western blot assays, respectively.

Statistical analysis. Data are expressed as the mean ± standard deviation (SD) from at least three independent experiments. Statistical significance among groups was assessed with unpaired Student's t-test and two-way ANOVA followed by Sidak's multiple comparisons test. A P-value of <0.05 was considered as indicative of a statistically significant difference. All statistical analyses were performed using GraphPad Prism version 8.0.1 (GraphPad Software, Inc.).

Results

CD9 activates PI3K/AKT signaling. To study the effect of CD9 on the PI3K/AKT pathway, we assessed activation of the pathway in a CD9-knockdown B-ALL cell line SUP-B15. We used the lentiviral-mediated shRNA approach in SUP-B15 cells to establish an efficient permanent method of downregulating the expression of CD9. Lentiviral delivery of shRNA targeted against *CD9* led to a significantly downregulation of *CD9* mRNA in SUP-B15 cells, as measured by RT-qPCR (Fig. S1). ELISA results showed that the level of p-PI3K protein was significantly reduced in the SUP-B15 cells transduced with the PHY-310 lentiviral vector containing shRNA targeting *CD9* (SUP-B15-shCD9 group) compared with wide-type SUP-B15 cells (SUP-B15-WT group) and those cells transduced with a blank PHY-310 vector (SUP-B15-shControl group; Fig. 1A). In addition, western blot analysis revealed a significant reduction in the p-AKT/AKT ratio in SUP-B15 cells after *CD9* knockdown (Fig. 1B and C). In addition to p-PI3K and p-AKT, we also tested their downstream targets, including drug resistance-(such as P-gp, MRP1 and BCRP) and cell motility-related molecules (such as MMP2 and p-FAK), by western blotting in SUP-B15 cells after *CD9* knockdown. Silencing of *CD9* significantly decreased P-gp, MRP1, BCRP, MMP2 expression and the p-FAK/FAK ratio (Fig. 1B and C).

CD9 interacts directly with PI3K-p85. To confirm the interaction between CD9 and PI3K-p85, we constructed GST-PI3K-p85α and GST-PI3K-p85β prokaryotic expression vectors, as well as MYC-CD9 mammalian expression vector. Using these vectors we assessed the interaction between CD9 protein and either PI3K-p85α or PI3K-p85β by GST pull-down assay. Successful transfection of 293T cells with the *CD9* expression plasmid was confirmed by western blot analysis (Fig. S2). As shown in Fig. 2, MYC-CD9 recombinant protein was able to bind to either GST-PI3K-p85α or GST-PI3K-p85β fusion protein instead of the GST control protein, suggesting that CD9 directly binds to both PI3K-p85α and PI3K-p85β *in vitro*.

Since CD9 interacts directly with both PI3K-p85α and PI3K-p85β *in vitro*, we next investigated whether CD9 binds to PI3K-p85 *in vivo*. We constructed expression vectors for MYC-tagged CD9 as well as HA-tagged PI3K-p85α or PI3K-p85β. Successful transfection of 293T cells with *PI3K-p85α* expression plasmid or *PI3K-p85β* expression plasmid was confirmed by western blot analysis (Figs. S3 and 4). Then, MYC-CD9 expression vector and either the HA-PI3K-p85α or HA-PI3K-p85β expression vector were transfected into 293T cells and the cell extracts were subjected to the co-immunoprecipitation assay using an anti-MYC antibody. Both PI3K-p85α and PI3K-p85β were detected in immune complexes of MYC-CD9 (Fig. 3), supporting that CD9 interacts with both PI3K-p85α and PI3K-p85β *in vivo*.

The PI3K/AKT pathway inhibitor has in vitro anti-leukemia effects in SUP-B15 cells. Since CD9 is involved in the regulation of the biological behavior of B-ALL cells through the PI3K/AKT pathway, we furthermore investigated the anti-leukemia effects of the inhibition of the PI3K/AKT pathway in SUP-B15 cells using LY294002, a PI3K/AKT pathway inhibitor. The results showed that the PI3K/AKT inhibitor LY294002 mirrored the effects of *CD9* knockdown in SUP-B15 cells. Treatment with LY294002 inhibited cell proliferation (Fig. 4A) as well as increased the inhibitory response of SUP-B15 cells to VCR (Fig. 4B), DNR (Fig. 4C), CPM (Fig. 4D) and DXM (Fig. 4E), respectively. In addition, treatment with LY294002 inhibited adhesion (Fig. 4F), migration (Fig. 4G) and invasion (Fig. 4H) of SUP-B15 cells. To test the effect of LY294002 on the expression of p-PI3K, ELISA was performed after exposure to the compound for 24 h. The protein level of p-PI3K was significantly reduced after treatment with LY294002 (Fig. 5A). Western blot assay also showed a reduction in the p-AKT/AKT ratio by LY294002 treatment (Fig. 5B and C), suggesting that PI3K/AKT signaling was inhibited. Additionally, the treatment with LY294002 increased the protein levels of p53, p21 and cleaved caspase-3, while decreasing P-gp, MRP1, BCRP, MMP-2 expression and the p-FAK/FAK ratio (Fig. 5B and C).

Discussion

As a commonly expressed immunophenotypic marker of B-ALL, CD9 is found to regulate the biological behavior of B-ALL cells and to be associated with the clinical prognosis of B-ALL patients (2-7). However, the corresponding mechanisms underlying the effects of CD9 on the disease progression of B-ALL remain to be explored. The PI3K/AKT signaling pathway is shown to be involved in a variety of tumor-related biological functions, and its role in tumorigenesis and development is also well-established (8). It should be noted that previously published experimental studies have demonstrated that tetraspanin proteins are capable of regulating the PI3K/AKT pathway. We therefore hypothesized that CD9 may be involved in the regulation of the biological behavior of B-ALL cells through the PI3K/AKT pathway. In order to investigate the relationship between CD9 and the PI3K/AKT pathway, we determined the expression of p-PI3K and p-AKT in B-ALL cell line SUP-B15 after *CD9* knockdown. Results showed that p-PI3K expression and the p-AKT/AKT ratio in the SUP-B15 cells was significantly reduced after *CD9* knockdown, suggesting that CD9 regulates the activity of PI3K/AKT signaling pathway.

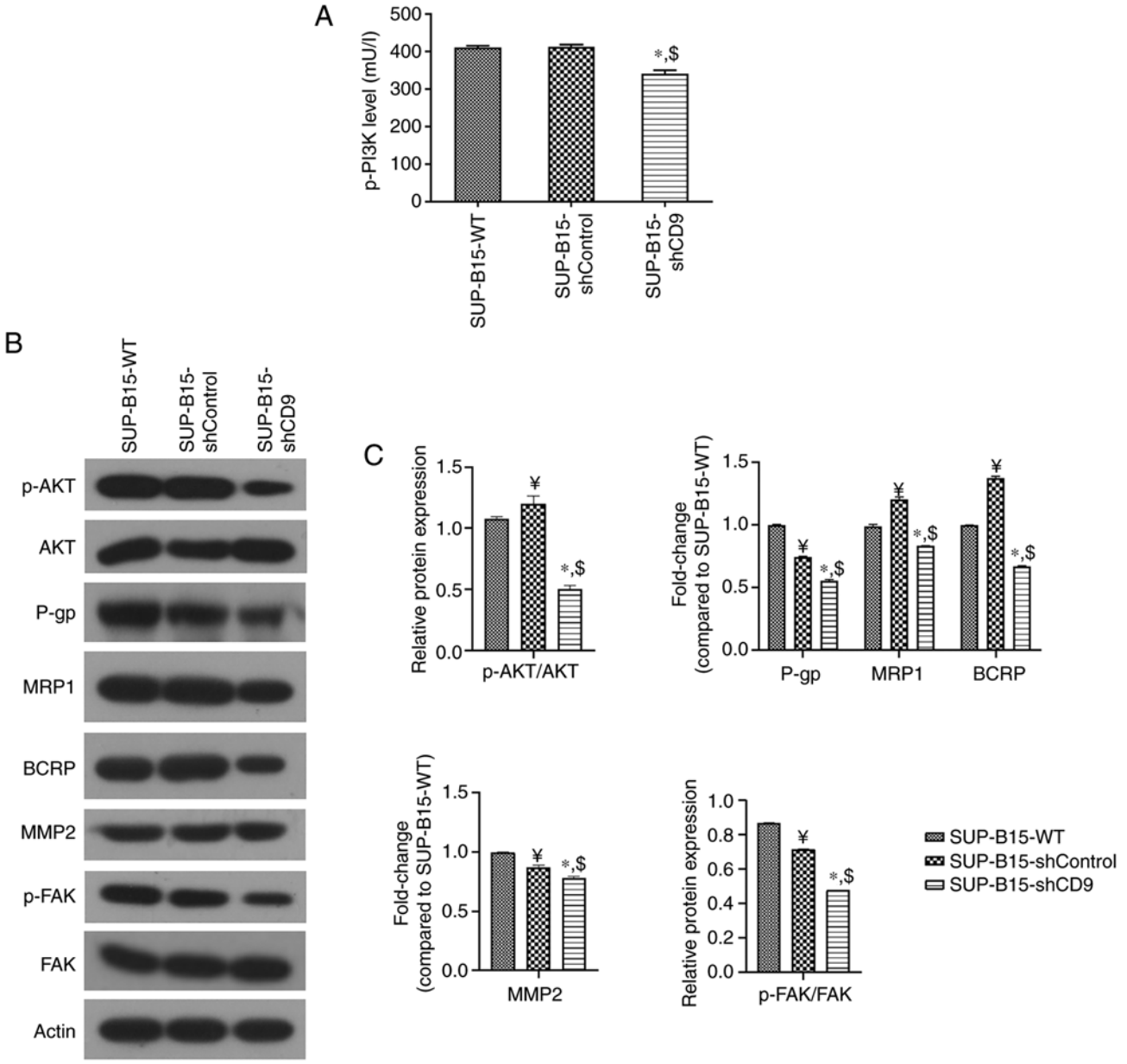

Figure 1. *CD9* knockdown suppresses the PI3K/AKT pathway. (A) ELISA was used to measure the expression of p-PI3K. (B) Western blot analysis was used to detect the protein levels of p-AKT, as well as drug-resistance-related (P-gp, MRP1 and BCRP) and motility-related factors (MMP2 and p-FAK). β-actin was used as the loading control. (C) Densitometry results are expressed as fold change against untreated control (normalized to the density of the corresponding β-actin band), or the ratio of phosphoprotein to total protein. SUP-B15-WT represents the wild-type SUP-B15 cells; SUP-B15-shControl represents the SUP-B15 cells transduced with a blank PHY-310 vector; SUP-B15-shCD9 represents the SUP-B15 cells transduced with the PHY-310 lentiviral vector containing shRNA targeting *CD9*; $^{¥}$P<0.05 vs. SUP-B15-WT group; *P<0.05 vs. SUP-B15-WT group; $^{\$}$P<0.05 vs. SUP-B15-shControl group. p-PI3K, phosphorylated-phosphatidylinositol-3 kinase; p-AKT, phosphorylated-protein kinase B; P-gp, P-glycoprotein; MRP1, multidrug resistance-associated protein 1; BCRP, breast cancer resistance protein; MMP2, matrix metalloproteinase 2; p-FAK, phosphorylated-focal adhesion kinase.

The PI3K/AKT pathway has been shown to be involved in the regulation of cell proliferation and apoptosis via its downstream cell cycle- and apoptosis-related molecules, such as p53, p21 and cleaved caspase-3 (12-14). Importantly, our previous study demonstrated that silencing of *CD9* upregulated the protein levels of p53, p21 and cleaved caspase-3 in SUP-B15 cells, which may result in the suppression of cell cycle progression and induction of apoptosis in SUP-B15 cells (7). Additionally, the downregulation of CD9 expression was found to increase the cytotoxicity of chemotherapeutic agents in SUP-B15 cells (7). Although the drug-resistance of tumor cells is quite complex, factors that may be involved, such as ATP-binding cassette drug transporters P-gp, MRP1 and BCRP, have been identified. More relatively, the activation of the PI3K/AKT pathway has been reported to contribute to drug-resistance of tumor cells through the upregulation of ATP-binding cassette drug transporters (15). Similarly, the present results indicated that the downregulation of CD9 expression significantly reduced the protein levels of P-gp, MRP1 and BCRP in SUP-B15 cells, suggesting that the CD9-regulated chemo-resistance of B-ALL cells may be mediated by ATP-binding cassette drug transporters, downstream targets of the PI3K/AKT pathway.

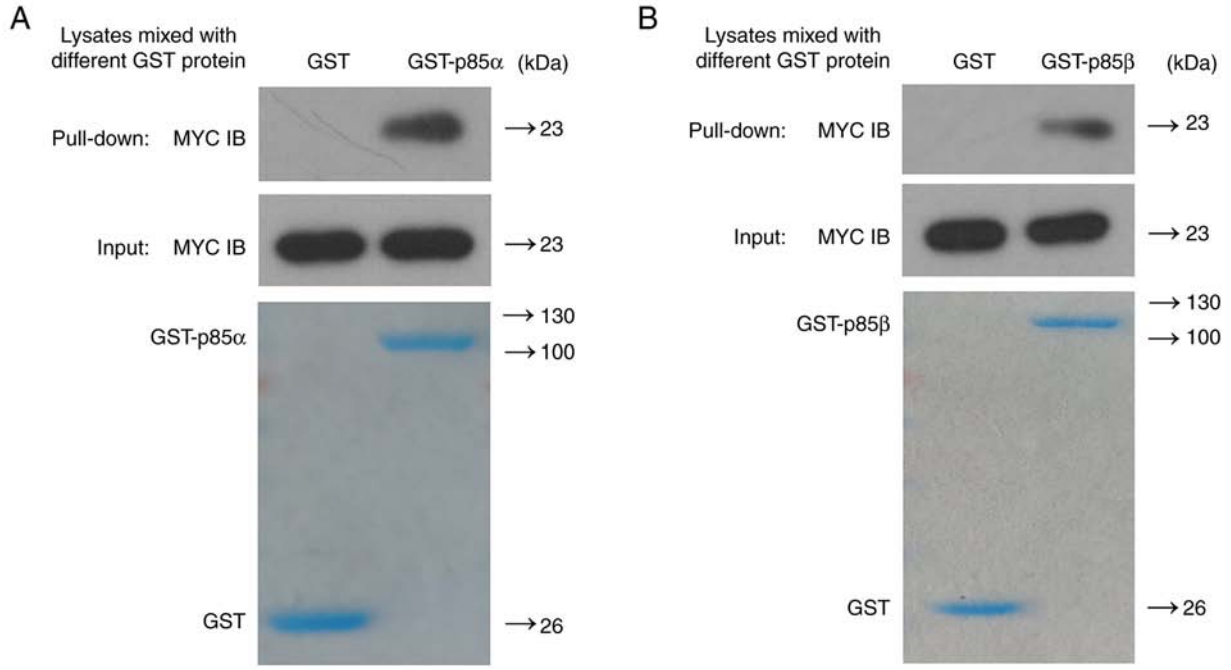

Figure 2. 293T cells were transfected with MYC-CD9 expression vector. Lysates from the transfected cells were mixed with either (A) GST-PI3K-p85α or (B) GST-PI3K-p85β fusion protein, and interaction between CD9 and the GST proteins was assessed by GST pull-down assay. Binding complexes were subjected to immunoblotting (IB) analysis with an antibody against MYC (pull-down panels). A total of 10% of the transfected cell lysates was examined by IB with an anti-MYC antibody to document the amount of CD9 protein used in the GST pull-down assay (input panels). GST-PI3K-p85α and GST-PI3K-p85β fusion proteins were purified and verified by GST beads and Coomassie blue staining (lowest panels).

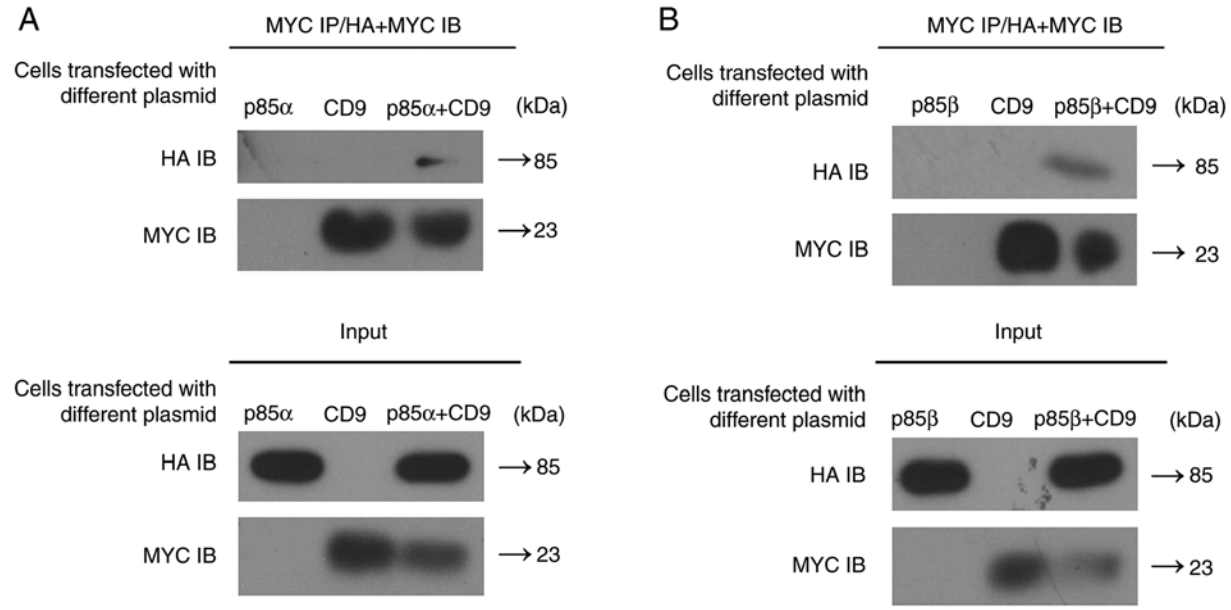

Figure 3. Co-immunoprecipitation of CD9 and either PI3K-p85α or PI3K-p85β. 293T cells were cotransfected with plasmids encoding MYC-CD9 and either HA-tagged PI3K-p85α or PI3K-p85β. Transfected cell lysates were immunoprecipitated (IP) with an anti-MYC antibody, and the immunoprecipitates were examined by immunoblotting (IB) with anti-HA or anti-MYC antibodies (upper panels). In the lower panels, transfected cell lysates were examined by IB with anti-HA or anti-MYC antibodies without prior immunoprecipitation. 293T cells transfected with plasmids encoding any MYC-CD9, HA-PI3K-p85α or HA-PI3K-p85β were used as the controls.

Metastasis and invasion are key clinicopathological features of acute leukemia (16). Our previous study demonstrated that downregulation of CD9 expression inhibited cell adhesion, migration and invasion in SUP-B15 cells (7). On the other hand, activation of the PI3K/AKT pathway has been shown to promote adhesion, migration and invasion of tumor cells by the upregulation of MMP2 and p-FAK (17-19). The present study indicated that *CD9* knockdown significantly reduced MMP2 expression and the p-FAK/FAK ratio in SUP-B15 cells, suggesting that the downregulation of CD9 expression

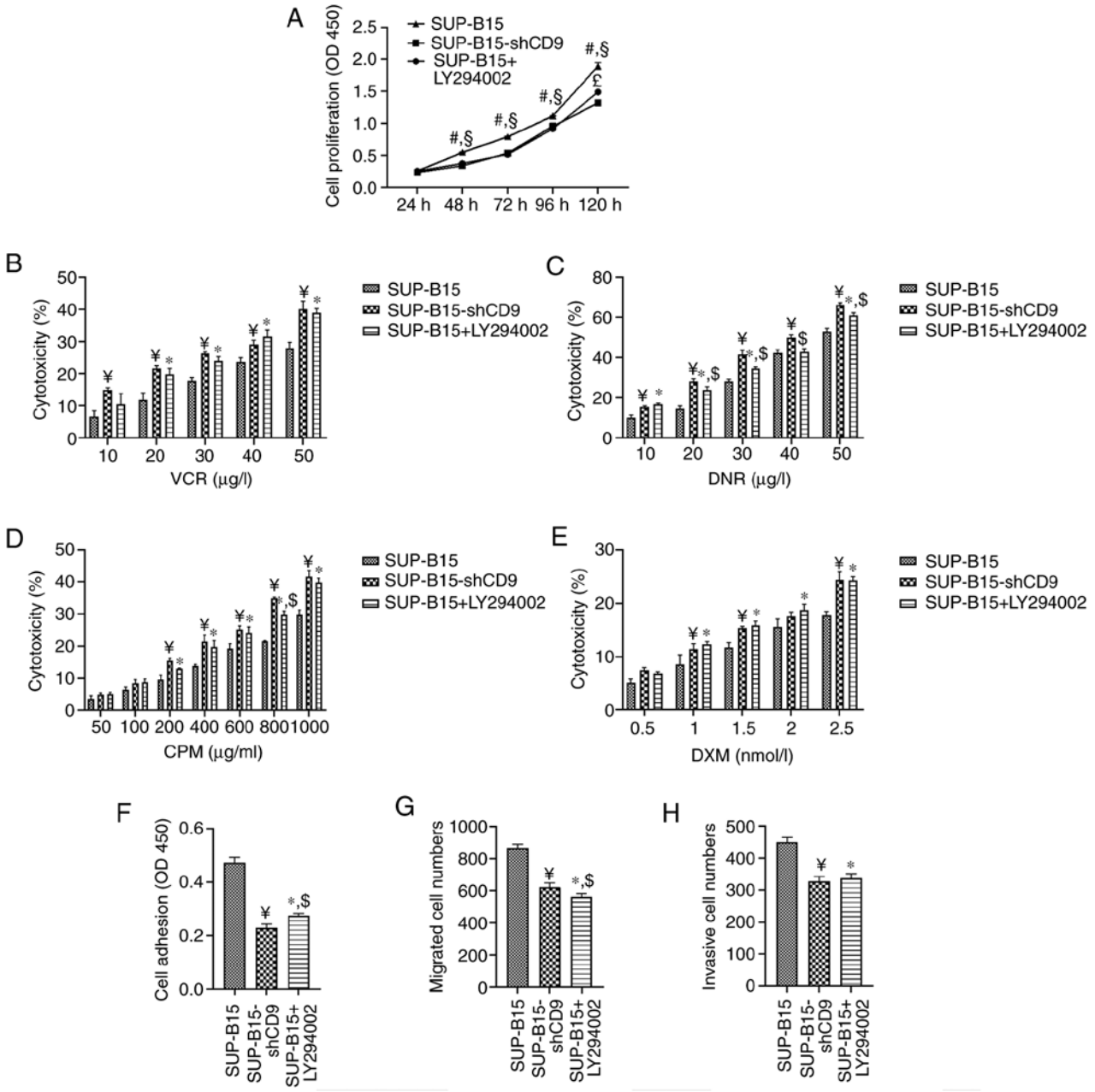

Figure 4. Treatment with PI3K/AKT inhibitor LY294002 suppresses cell proliferation, adhesion, migration and invasion, while increasing the cytotoxicity of chemotherapeutic agents in SUP-B15 cells. (A) Cell proliferation curves of SUP-B15 cells were measured by a CCK-8 assay. (B-E) SUP-B15 cells were treated with different concentration gradient of (B) VCR, (C) DNR, (D) CPM and (E) DXM for 48 h. CCK-8 assay was used to measure cell viability. (F) The adhesion ability of SUP-B15 cells was evaluated by cell adhesion to Superfibronectin. Adherent cells were quantified by CCK-8 assay. (G) The migration and (H) invasion ability of SUP-B15 cells was measured by the Transwell assay with uncoated or Matrigel-coated membranes. Migrated and invasive cells were counted by hemocytometer under a light microscope. SUP-B15-shCD9 represents the SUP-B15 cells transduced with the PHY-310 lentiviral vector containing shRNA targeting *CD9*; $^{\#}$P<0.05 vs. SUP-B15-shCD9 cells without LY294002 treatment; §P<0.05 vs. SUP-B15 cells treated with LY294002; $^{£}$P<0.05 vs. SUP-B15-shCD9 cells without LY294002 treatment; $^{¥}$P<0.05 vs. SUP-B15 cells without LY294002 treatment; *P<0.05 vs. SUP-B15 cells without LY294002 treatment; $^{\$}$P<0.05 vs. SUP-B15-shCD9 cells without LY294002 treatment; CCK-8, Cell Counting Kit-8; VCR, vincristine; DNR, daunorubicin; CPM, cyclophosphamide; DXM, dexamethasone; OD, optical density.

inhibited adhesion, migration and invasion of B-ALL cells by suppressing the expression of MMP2 and p-FAK through PI3K/AKT pathway.

PI3K, as a heterodimer composed of a p85-regulatory subunit and a p110-catalytic subunit, could be recruited to receptor tyrosine residues on the cell surface membrane and then be activated by either phosphorylation or binding of adaptor proteins to the Src Homlogy 2 domain of p85 subunit (20-25). As a commonly mutated protein in solid tumors, PI3K-p85 plays a key role in the activation of the PI3K/AKT pathway. Moreover, the downregulation of PI3K-p85 expression has been shown to inhibit proliferation and migration of tumor cells (26-29). We therefore hypothesized that CD9 may activate the PI3K/AKT pathway via the interaction with PI3K-p85. Two forms of PI3K-p85 have been identified: PI3K-p85α is ubiquitously expressed and is encoded by the *Pik3r1* gene, whereas PI3K-p85β is also widely expressed but is encoded by the *Pik3r2* gene (30,31). In the present study, GST pull-down

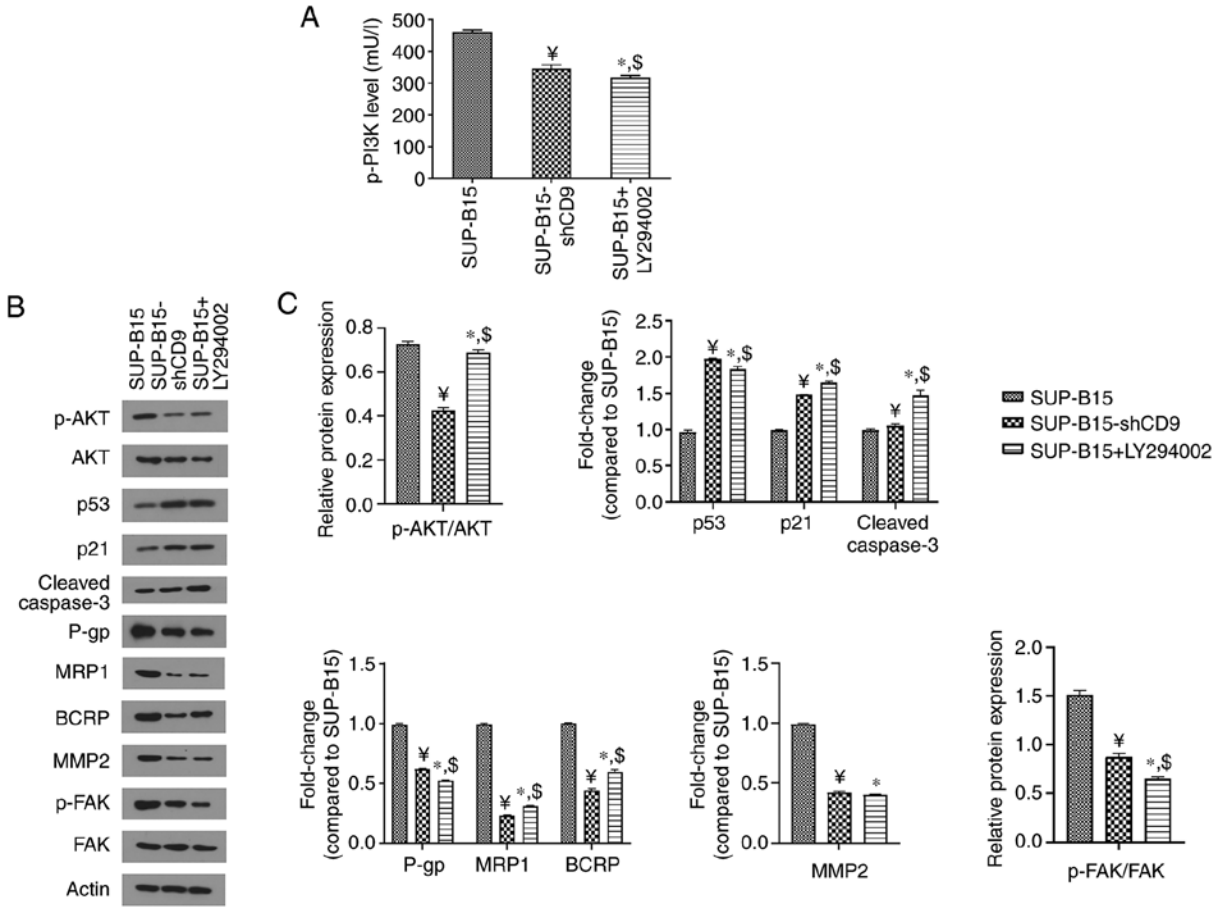

Figure 5. The treatment with PI3K/AKT inhibitor LY294002 suppresses the PI3K/AKT pathway. (A) ELISA was used to measure the expression of p-PI3K. (B) Western blot analysis was used to detect the protein levels of p-AKT, as well as cell cycle- and apoptosis-related (including p53, p21 and cleaved caspase-3), drug-resistance-related (including P-gp, MRP1 and BCRP) and motility-related factors (including MMP2 and p-FAK). β-actin was used as the loading control. (C) Densitometry results are expressed as fold change against untreated control (normalized to the density of the corresponding β-actin band), or the ratio of phosphoprotein to total protein. SUP-B15-shCD9 represents the SUP-B15 cells transduced with the PHY-310 lentiviral vector containing shRNA targeting *CD9*; ¥P<0.05 vs. SUP-B15 cells without LY294002 treatment; *P<0.05 vs. SUP-B15 cells without LY294002 treatment; $P<0.05 vs. SUP-B15-shCD9 cells without LY294002 treatment. p-PI3K, phosphorylated-phosphatidylinositol-3 kinase; p-AKT, phosphorylated-protein kinase B; P-gp, P-glycoprotein; MRP1, multidrug resistance-associated protein 1; BCRP, breast cancer resistance protein; MMP2, matrix metalloproteinase 2; p-FAK, phosphorylated-focal adhesion kinase.

assay showed the binding between CD9 and both PI3K-p85α and PI3K-p85β *in vitro*, while co-immunoprecipitation assay showed the binding between CD9 and both PI3K-p85α and PI3K-p85β *in vivo*. These results further indicated that CD9 could mediate proliferation, drug-resistance, adhesion, migration and invasion of B-ALL cells through activation of the PI3K/AKT pathway.

Furthermore, in order to assess the *in vitro* anti-leukemia effects of the inhibition of the PI3K/AKT pathway in B-ALL cells, LY294002 was used to culture SUP-B15 cells and thereby manipulate the PI3K/AKT pathway. Meanwhile, we investigated the effects of LY294002 treatment on the biological behavior as well as PI3K/AKT pathway in SUP-B15 cells. The present results showed that LY294002 treatment significantly inhibited cell proliferation, adhesion, migration and invasion, while promoting the efficacy of chemotherapeutic agents in SUP-B15 cells. We also found that LY294002 treatment significantly reduced p-PI3K expression and the p-AKT/AKT ratio, as well as drug-resistance-related (including P-gp, MRP1 and BCRP) and motility-related factors (including MMP2 and p-FAK), while increasing the protein levels of cell cycle- and apoptosis-related factors (including p53, p21 and cleaved caspase-3). These findings suggest that inhibition of the PI3K/AKT pathway may provide a novel treatment option for $CD9^+$ B-ALL.

In conclusion, this study demonstrated that CD9 could modulate the biological behavior of B-ALL cells through the PI3K/AKT singling pathway via direct interaction with PI3K-p85, and the inhibition of PI3K/AKT pathway might be a novel treatment option for $CD9^+$ B-ALL. Further studies are needed to verify the efficiency of the PI3K/AKT inhibitor in patient-derived primary B-ALL cells and xenograft animal models for B-ALL.

Acknowledgements

Not applicable.

Funding

This research was funded by the Natural Science Foundation of Zhejiang Province (grant nos. LY21H080006 and LQ19H080002), and the Public Welfare Science and Technology Project of Wenzhou (grant no. Y20190119).

Availability of data and materials

The datasets generated or analyzed during this study are not publicly available due to confidentiality of another study from our group but are available from the corresponding authors upon reasonable request.

Authors' contributions

JHF and KTL conceived of the research project. YFS, ZYH, YSH, RJD, CYX and KY conducted the experiments and collected the data. JHF, KTL and YHS analyzed the data. YFS and ZYH wrote the paper. All authors read and approved the manuscript and agree to be accountable for all aspects of the research in ensuring that the accuracy or integrity of any part of the work are appropriately investigated and resolved.

Ethics approval and consent to participate

Not applicable.

Patient consent for publication

Not applicable.

Competing interests

The authors declare that they have no competing interests.

References

1. Hemler ME: Tetraspanin functions and associated microdomains. Nat Rev Mol Cell Biol 6: 801-811, 2005.
2. Liang P, Miao M, Liu Z, Wang H, Jiang W, Ma S, Li C and Hu R: CD9 expression indicates a poor outcome in acute lymphoblastic leukemia. Cancer Biomark 21: 781-786, 2018.
3. Leung KT, Zhang C, Chan KYY, Li K, Cheung JTK, Ng MHL, Zhang XB, Sit T, Lee WYW, Kang W, *et al*: CD9 blockade suppresses disease progression of high-risk pediatric B-cell precursor acute lymphoblastic leukemia and enhances chemosensitivity. Leukemia 34: 709-720, 2020.
4. Nishida H, Yamazaki H, Yamada T, Iwata S, Dang NH, Inukai T, Sugita K, Ikeda Y and Morimoto C: CD9 correlates with cancer stem cell potentials in human B-acute lymphoblastic leukemia cells. Biochem Biophys Res Commun 382: 57-62, 2009.
5. Yamazaki H, Xu CW, Naito M, Nishida H, Okamoto T, Ghani FI, Iwata S, Inukai T, Sugita K and Morimoto C: Regulation of cancer stem cell properties by CD9 in human B-acute lymphoblastic leukemia. Biochem Biophys Res Commun 409: 14-21, 2011.
6. Arnaud MP, Vallee A, Robert G, Bonneau J, Leroy C, Varin-Blank N, Rio AG, Troadec MB, Galibert MD and Gandemer V: CD9, a key actor in the dissemination of lymphoblastic leukemia, modulating CXCR4-mediated migration via RAC1 signaling. Blood 126: 1802-1812, 2015.
7. Xing C, Xu W, Shi Y, Zhou B, Wu D, Liang B, Zhou Y, Gao S and Feng J: CD9 knockdown suppresses cell proliferation, adhesion, migration and invasion, while promoting apoptosis and the efficacy of chemotherapeutic drugs and imatinib in Ph+ ALL SUP-B15 cells. Mol Med Rep 22: 2791-2800, 2020.
8. Fruman DA, Chiu H, Hopkins BD, Bagrodia S, Cantley LC and Abraham RT: The PI3K pathway in human disease. Cell 170: 605-635, 2017.
9. Sugiura T and Berditchevski F: Function of alpha3beta1-tetraspanin protein complexes in tumor cell invasion. Evidence for the role of the complexes in production of matrix metalloproteinase 2 (MMP-2). J Cell Biol 146: 1375-1389, 1999.
10. Sawada S, Yoshimoto M, Odintsova E, Hotchin NA and Berditchevski F: The tetraspanin CD151 functions as a negative regulator in the adhesion-dependent activation of Ras. J Biol Chem 278: 26323-26326, 2003.
11. Qi JC, Wang J, Mandadi S, Tanaka K, Roufogalis BD, Madigan MC, Lai K, Yan F, Chong BH, Stevens RL and Krilis SA: Human and mouse mast cells use the tetraspanin CD9 as an alternate interleukin-16 receptor. Blood 107: 135-142, 2006.
12. Zhang L, Zhu S, Shi X and Sha W: The silence of p66(Shc) in HCT8 cells inhibits the viability via PI3K/AKT/Mdm-2/p53 signaling pathway. Int J Clin Exp Pathol 8: 9097-9104, 2015.
13. Tang C, Lu YH, Xie JH, Wang F, Zou JN, Yang JS, Xing YY and Xi T: Downregulation of survivin and activation of caspase-3 through the PI3K/Akt pathway in ursolic acid-induced HepG2 cell apoptosis. Anticancer Drugs 20: 249-258, 2009.
14. Abbas T and Dutta A: p21 in cancer: Intricate networks and multiple activities. Nat Rev Cancer 9: 400-414, 2009.
15. Wang H, Jia XH, Chen JR, Yi YJ, Wang JY, Li YJ and Xie SY: HOXB4 knockdown reverses multidrug resistance of human myelogenous leukemia K562/ADM cells by downregulating P-gp, MRP1 and BCRP expression via PI3K/Akt signaling pathway. Int J Oncol 49: 2529-2537, 2016.
16. Klein G, Vellenga E, Fraaije MW, Kamps WA and de Bont ES: The possible role of matrix metalloproteinase (MMP)-2 and MMP-9 in cancer, e.g. acute leukemia. Crit Rev Oncol Hematol 50: 87-100, 2004.
17. Zhou R, Xu L, Ye M, Liao M, Du H and Chen H: Formononetin inhibits migration and invasion of MDA-MB-231 and 4T1 breast cancer cells by suppressing MMP-2 and MMP-9 through PI3K/AKT signaling pathways. Horm Metab Res 46: 753-760, 2014.
18. Yadav V and Denning MF: Fyn is induced by Ras/PI3K/Akt signaling and is required for enhanced invasion/migration. Mol Carcinog 50: 346-352, 2011.
19. Tai YL, Chen LC and Shen TL: Emerging roles of focal adhesion kinase in cancer. Biomed Res Int 2015: 690690, 2015.
20. Cantley LC: The phosphoinositide 3-kinase pathway. Science 296: 1655-1657, 2002.
21. Di Zazzo E, Feola A, Zuchegna C, Romano A, Donini CF, Bartollino S, Costagliola C, Frunzio R, Laccetti P, Di Domenico M and Porcellini A: The p85 regulatory subunit of PI3K mediates cAMP-PKA and insulin biological effects on MCF-7 cell growth and motility. ScientificWorldJournal 2014: 565839, 2014.
22. Breitkopf SB, Yang X, Begley MJ, Kulkarni M, Chiu YH, Turke AB, Lauriol J, Yuan M, Qi J, Engelman JA, *et al*: A cross-species study of pi3k protein-protein interactions reveals the direct interaction of P85 and SHP2. Sci Rep 6: 20471, 2016.
23. Lee JY, Chiu YH, Asara J and Cantley LC: Inhibition of PI3K binding to activators by serine phosphorylation of PI3K regulatory subunit p85alpha Src homology-2 domains. Proc Natl Acad Sci USA 108: 14157-14162, 2011.
24. Comb WC, Hutti JE, Cogswell P, Cantley LC and Baldwin AS: p85α SH2 domain phosphorylation by IKK promotes feedback inhibition of PI3K and Akt in response to cellular starvation. Mol Cell 45: 719-730, 2012.
25. Hofmann BT and Jücker M: Activation of PI3K/Akt signaling by n-terminal SH2 domain mutants of the p85α regulatory subunit of PI3K is enhanced by deletion of its c-terminal SH2 domain. Cell Signal 24: 1950-1954, 2012.
26. Jaiswal BS, Janakiraman V, Kljavin NM, Chaudhuri S, Stern HM, Wang W, Kan Z, Dbouk HA, Peters BA, Waring P, *et al*: Somatic mutations in p85alpha promote tumorigenesis through class IA PI3K activation. Cancer Cell 16: 463-474, 2009.
27. Folgiero V, Di Carlo SE, Bon G, Spugnini EP, Di Benedetto A, Germoni S, Pia Gentileschi M, Accardo A, Milella M, Morelli G, *et al*: Inhibition of p85, the non-catalytic subunit of phosphatidylinositol 3-kinase, exerts potent antitumor activity in human breast cancer cells. Cell Death Dis 3: e440, 2012.
28. Sun M, Hillmann P, Hofmann BT, Hart JR and Vogt PK: Cancer-derived mutations in the regulatory subunit p85alpha of phosphoinositide 3-kinase function through the catalytic subunit p110alpha. Proc Natl Acad Sci USA 107: 15547-15552, 2010.
29. Feola A, Cimini A, Migliucci F, Iorio R, Zuchegna C, Rothenberger R, Cito L, Porcellini A, Unteregger G, Tombolini V, *et al*: The inhibition of p85αPI3KSer83 phosphorylation prevents cell proliferation and invasion in prostate cancer cells. J Cell Biochem 114: 2114-2119, 2013.
30. Fruman DA, Snapper SB, Yballe CM, Davidson L, Yu JY, Alt FW and Cantley LC: Impaired B cell development and proliferation in absence of phosphoinositide 3-kinase p85alpha. Science 283: 393-397, 1999.
31. Terauchi Y, Tsuji Y, Satoh S, Minoura H, Murakami K, Okuno A, Inukai K, Asano T, Kaburagi Y, Ueki K, *et al*: Increased insulin sensitivity and hypoglycaemia in mice lacking the p85 alpha subunit of phosphoinositide 3-kinase. Nat Genet 21: 230-235, 1999.